大韓土木學會論文集
第13卷 第1號 · 1993年 3月
pp. 65~74

보강된 적층평판의 최적화 설계

Design Optimization of Blade Stiffened Laminated Composite Plates

신 영 석*
Shin, Yung Seok

Abstract

The buckling load of a blade stiffened laminated composite plate having midplane symmetry is maximized for a given total weight. The thicknesses of the layers and the width and height of the stiffener are taken as the design variables. Buckling analysis is carried out using a finite element method. The optimization problem is solved using an IMSL subroutine. Due to the highly nonlinear nature of the optimality equations, several local optimum solutions are found. Various combinations of fiber orientation for the laminate layers and the blade stiffener are investigated to examine their relative efficiency. Out of several cases examined, the best design was produced from the combination of $(0^0\text{Beam}/0^0/90^0)$s.

요 지

중립축에 대하여 대칭인 보강된 적층평판의 좌굴하중을 극대화 하는 최적설계를 시도하였다. 전체 평판의 무게가 일정한 가운데 적층평판을 이루는 각기 판의 두께와 보강재의 단면을 이루는 두께와 높이를 설계변수로 취하였다. 유한요소법을 이용하여 평판의 좌굴하중이 계산되었으며 최적설계는 IMSL program routine을 사용하였다. 최적설계시 나타나는 optimality condition이 고도의 비선형 연립방정식이 되므로 이경우 여러개의 국부 최적점이 발견되었다. 보강재와 평판의 각층에서의 보강섬유의 방향을 달리하며 각자의 효율성을 연구 조사하였으며 이중$(0^0\text{Beam}/0^0/90^0)$s의 경우에 가장 우수한 설계를 할수 있는것으로 나타났다.

1. INTRODUCTION

Composite materials are popularly used as the structural material in these days because of their high strength-to-weight and stiffness-to-weight ratios. These properties are very important in many of today's engineered structures where high strength is required but a severe penally is incurred for added weight. Previous works in the area of design optimization of composite plates, have focused on flat plates without stiffeners. Recently, laminated plates stiffened by longitudinal members became common structural components and received more attentions for the design optimization[1,4]. The biggest advantage of the stiffeners is the increased bending stiffness of the panel with a minimum of additional materials, which

* 정회원 · 아주대학교 토목공학과, 조교수.

makes these structures highly desirable for out-of-plane loads or in-plane buckling loads. However, the complex geometry of the stiffened plates makes it difficult to adopt the simplifying assumptions used for flat laminates which often lead to closed form solutions.

The present study focuses on the optimal design of laminated composite blade-stiffened laminate for the maximum buckling load. Specifically, it deals with a symmetric blade stiffened composite plate that has n number of laminae and a stiffener on either side of the midplane. A symmetric composite plate is chosen so that the coupling between extenseon and bending is eliminated. This lack of coupling allows the use of linear buckling analysis for the buckling load. The buckling analysis is performed using a finite element method. The design objective in this study is to maximize the buckling load with a given total material constraint. Design variables are set to the laminae thicknesses and the stiffener height and the width. The fiber orientation of the laminae and the stiffener are allowed to be either 0^0 or 90^0. Four different stacking sequences of the fiber orientation are investigated. For each case, design optima are investigated. These optima are then compared to determine the best stacking sequence. The study is completed for two different cases of total material volume.

STIFFENED COMPOSITE PLATE

The plate considered in this study is square and simply supported along all four edges as shown in Figure 1. The plate has a symmetric (top and bottom) blade stiffener at center and is subjected to in-plane loads in the X-direction. Two forms of plate buckling are considered: the plate and stiffener, as one unit, can buckle in an overall buckling mode; and the blade stiffener in itself can undergo local buckling. The buckling analyses of these two are performed separately. For the case of overall plate buckling, the blade stiffener is treated as a beam reinforcing the plate. A finite element formulation is used, and the stiffness matrix and the geometric stiffness matrix of the

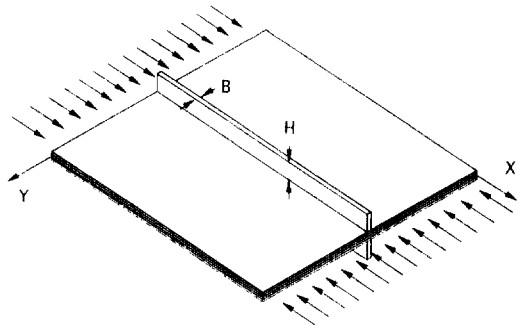

Fig. 1. Stiffened plate under inplane load.

beam are calculated and combined with the corresponding matrices of the base plate. For the case of local stiffener buckling, the blade stiffener is treated as an independent plate subject to an in-plane compressive load. Assuming that three sides are simply supported and the fourth side is free, we can obtain the local buckling load of the stiffener analytically.

Overall Plate Buckling Analysis

As the stiffener is treated as a beam, the governing differential equation is

$$(E_b I_b W'')'' - P_b W'' = 0 \tag{1}$$

where W is the transverse deflection of the beam, a prime (') denotes differentiation with respect to the longitudinal coordinate X, and Pb is the beam axial load. Young's modulus of the beam in longitudinal direction is denoted by Eb, and the second moment of inertia of the beam is denoted by Ib and can be expressed as follows:

$$I_b = \frac{2}{3} B\{(H+T_T)^3 - T_T^3\} \tag{2}$$

where B is the width, H is the height of the stiffener and TT is half the total thickness of the laminate plate on which the stiffener is placed (see Figure 1 and Figure 2). The factor of 2 in the expression for Ib accounts for the two stiffeners, one on top, and one on bottom of the plate. Each of the geometric quantities and material properties can be normalized dividing by the span length, L, or the layer stiffness of plate in fiber

direction, E11, as follows:

$$b=\frac{B}{L}\quad h=\frac{H}{L}\quad t_T=\frac{T_T}{L}\quad i_b=\frac{I_b}{L^4}=\frac{2}{3}b\{(h+t_T)^3-t_T^3\}$$

$$e_b=\frac{E_b}{E_{11}}\quad w=\frac{W}{L}\quad x=\frac{X}{L}\quad p_b=\frac{1}{E_{11}L^2}P_b \tag{3}$$

Then, we get the differential equation (1) also in nondimensional form:

$$(e_b i_b w'')''-p_b w''=0 \tag{4}$$

The finite element discretization of the above beam equation leads to

$$[K]_b\{U\}_b-p_b[K_G]_b\{U\}_b=0 \tag{5}$$

where $[K]_b$ is the global beam stiffness matrix, $[K_G]_b$ is the global beam geometric stiffness matrix, and $\{U\}_b$ is the generalized global displacement vector of the beam which has 2 degrees of freedom $\{w, \frac{dw}{x}\}$ at esch node.

For the plate buckling analysis, a 16 degree-of-freedom plate finite element[5] is used yielding the equation,

$$[K]\{U\}-n_x[K_G]\{U\}=0 \tag{6}$$

where $[K]$ is the global plate stiffness matrix, $[K_G]$ is the global plate geometric stiffness matrix, and $\{U\}$ is the generalized global displacement vector of the plate which has 4 degrees of freedom

$$\{w, \frac{\partial w}{\partial x}, \frac{\partial w}{\partial y}, \frac{\partial^2 w}{\partial x \partial y}\} \text{ at each node.}$$

Since the terms w and $\frac{dw}{dx}$ of the vector $\{U\}_b$ in equation(5) are equivalent to the terms w and $\frac{\partial w}{\partial x}$ in the vector $\{U\}$ equation(6), these two equations can be combined to get one matrix equation for overall buckling of the plate and stiffener. The overall equation is

$$[K\rangle\{U\}+[\underline{K}]_b\{U\}-n_x[K_G]\{U\}-p_b[\underline{K_G}]_b\{U\}=0 \tag{7}$$

where $[K]$ and $[K]_b$ are the plate and the beam stiffness matrix, respectively, $[K_G]$ and $[K_G]b$ are the plate and beam geometric stiffness matrix, respectively. The matrices $[K]_b$ and $[K_G]b$ are transformed from the matrices $[K]_b$ and $[K_G]_b$ to fit into the generalized displacement vector of plate $\{U\}$. The load carried by the beam is pb and the load carried by the plate is nx. These loads are proportional to the extensional stiffness of each. So the total load P on the stiffened plate is distributed as pg_1 to the plate and pg_2 to the stiffener, where g_1 and g_2 are expressed as follows:

$$g_1=\frac{e_p s_p}{e_p s_p+e_b s_b}$$

$$g_2=\frac{e_b s_b}{e_p s_p+e_b s_b} \tag{8}$$

where s_p and s_b are the nondimensional cross-sectional area of plate and beam, and e_p and e_b are the nondimensional elastic moduli of the laminated plate and the beam. The expression for e_p are obtained from

$$\frac{1}{e_p}\quad\frac{a_{22}a_{66}-a_{26}^2}{|[a]|}\,t_t \tag{9}$$

where $[a]$ is the nondimensional stretching stiffness matrix expressed as (see Figure 2)

$$[a]=2\sum_{k=1}^{n}[q]_k(z_k-z_{k+1}) \tag{10}$$

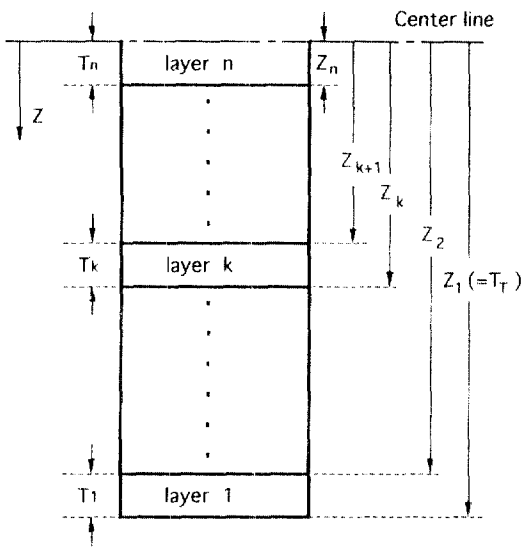

Fig. 2. Geometry of half of a 2n-layered symmetric laminate

In above equation, n is half the numper of total layers in plate, $\bar{q}$ is the nondimensional reduced stiffness of the laminate, and z_k is the nondimensional distance of each layer measured from the center of the laminate. Equation (7) may be written now as

$$[K]\{U\}+[\underline{K}]_b\{U\}-p(g_1[K_G]\{U\}-g_2[\underline{K}_g]_b\{U\})=0 \tag{11}$$

Now the overall buckling equation can be written in the form,

$$[K]_T\{U\}-p[K_G]_T\{U\}=0 \tag{12}$$

where $[K]_T$ is the total stiffness of the plate and stiffener combination and $[K_G]_T$ is the total geometric stiffness of the plate and stiffener combination. This generalized eigenvalue problem is solved using the DNLASO subroutine from the package LASO2 [6], which computes a few eigenvalues and associated eigenvectors of a large (sparse) symmetric matrix using a Lanczos algorithm [7].

Stiffener Local Buckling Analysis

The local buckling of the stiffener is analyzed separately from the overall plate analysis. The stiffener is treated as a plate which is simply supported at 3 edges(X=0, X=L, Z=0)and is free at one edge(Z=H). It is subject to axial compressive load Ps. Because two opposite sides are simply supported, this problem can be solved analytically. The governing partial differential equation for the orthotropic plate buckling problem is given from [8] as

$$D_{11}\frac{\partial^2 V}{\partial x^4}+22(D_{12}+2D_{66})\frac{\partial^4 V}{\partial x^2\partial Z^2}+D_{22}\frac{\partial^4 V}{\partial Z^4}-P_s\frac{\partial^2 V}{\partial Z^2}=0, \tag{13}$$

where V is the plate deflection, D_{ij} are the components of the bending stiffness matrix, and Ps refers to the stiffener local buckling load. By applying the boundary conditions and assuming a Levy's solution of the form,

$$V=\sum_{m=1,3,5\cdots}^{\infty} F(Z)m\ \sin\frac{m\pi x}{L} \tag{14}$$

the bucking load P_b can be solved directly and the nondimensional buckling load p_s is obtained from the relation

$$p_s=\frac{1}{E_{11}L}P_s. \tag{15}$$

OPTIMIZATION PROBLEM

The optimization problem is to maximize the buckling load of the blade stiffened plate for a given total material volume (which is proportional to the total weight). The design variables are set to the nondimensional thickness of the individual lamina, t_i, and the nondimensional width and height of the stiffener. Here the nondimensional width, b, and the nondimensional height, h, of the stiffener are denoted as t_n+1 and t_n+2, respectively. The nondimensional design variables, t_i, are subject to side constraints of

$$t_{i\ min} \le t_i \le t_{i\ max} \text{ for } i=1,2,\cdots,(n+2), \tag{16}$$

where t_i max and t_i min are upper and lower bounds on the design variables, respectively, and n is half the number of layers for the symmetric laminate.

The optimization problem for maximizing the buckling load is written as

$$\begin{aligned} &\max\ \beta \\ &\beta,\ t_i \\ &\text{such that } p_1 \ge \beta \\ &\qquad 0.999p_2 \ge \beta \\ &\qquad 0.998p_3 \ge \beta \\ &\qquad p_s \ge \beta \\ &\qquad 2\sum_{i=1}^{n}(\tau_i)+2t_{n+1}t_{n-2}-\theta=0 \\ &\quad \text{and}\quad t_{i\ min} \le t_i \le t_{i\ max} \text{ for } i=1,2,\cdots,(n+2), \end{aligned} \tag{17}$$

where p_1, p_2, and p_3 are the first three overall buckling loads of the stiffened plate which are obtained from overall FEM analysis, p_s is the local buckling load of the stiffener obtained analytically, and θ is the nondimensional total plate volume. The variable β is introduced to avoid having to

maximize the minimum of p_1, p_2, p_3, and p_s which is not a smooth function. The coefficients of 0.999, and 0.998 in the second and third constraints, are necessary to keep the eigenvalues p_1, p_2, and p_3 distinct when the buckling mode is bimodal or trimodal, and allow the calculation of derivatives of these buckling loads.

The above optimization problem is solved using one of the IMSL subroutine DNCONG that is used for general nonlinear programming problems. The subroutine DNCONG is based on subroutine NLPQL which uses a successive quadratic programming method with analytical gradients [9].

RESULTS AND DISCUSSION

The laminate plate chosen in this study is square with span length L and has 4 symmetric layers. The material selected for the laminate and the stiffener is a high-stiffness graphite/epoxy composite. The material properties of this composite are: $E_{11}=31.0\times10^6$ psi(213.7 GPa), $E_{22}=3.4\times10^6$ psi (23.3 GPa), $G_{12}=0.75\times10^6$ psi (5.17 GPa), $V_{12}=0.28$. Design optimization results are obtained for two different total volume conditions($\theta=0.04$ and 0.015) and four different stacking sequences:

$(0^0\text{Beam}/90^0/0^0)$s
$(0^0\text{Beam}/0^0/90^0)$s
$(90^0\text{Beam}/90^0/0^0)$s
$(90^0\text{Beam}/0^0/90^0)$s

The minimum and the maximum thicknesses of each laminae are set to 0.001L and 0.2L, respectively. The same upper and lower limits are used for the stiffener width and height. For each configuration, the values of the design variables at the optimum are given. Also listed are the active buckling loads and corresponding buckling modes. All the results are presented in nondimensional form.

Case 1:
$\theta=0.04$ and Ply Orientation $(0^0\text{Beam}/90^0/0^0)$s

For this configuration, two different optimum solutions are found. They are listed in Table 1

Table 1. Results of $(0^0\text{Beam}/90^0/0^0)$s laminate for $\theta=0.04$

t_1	t_2	b	h	p	Active Buckling Loads
0.00732	0.01020	0.03801	0.06369	0.0002646	P_1, P_2, P_3, P_s
0.01521	0.00100	0.05794	0.06526	0.0002822	P_1, P_2, P_s

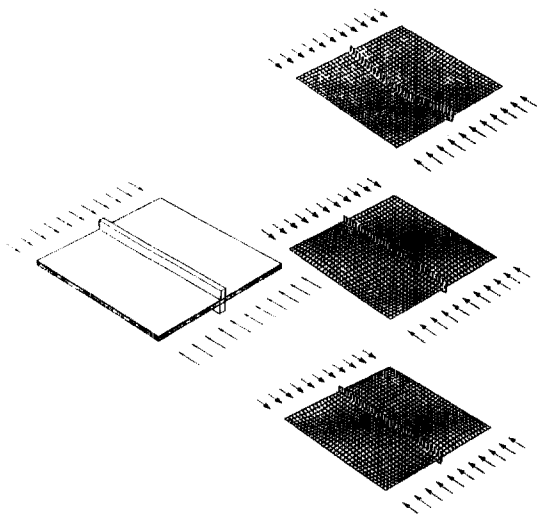

Fig. 3. Geometry and buckling modes of Case 1 for p=0.0002646.

below. Figures 3 and 4 show the scaled dimensions of the optimized plate and the overall plate buckling modes corresponding to the active buckling loads. Since all these modes have the same buckling load, actual buckling may occur in any linear combination of these multiple modes together with the local stiffener buckling.

Of the two optimal designs found for Case 1, the global optimum, which has higher buckling loads, is the one that has 3 active bucking loads. The design with 4 active buckling loads turns out to have lower buckling load and becomes the local optimum. Comparing these two designs, the global optimum is seen to increase the size of the stiffener and to decrease the thickness of the $t_2(0^0$ layer) to the lower limit. This causes a strong stiffe-

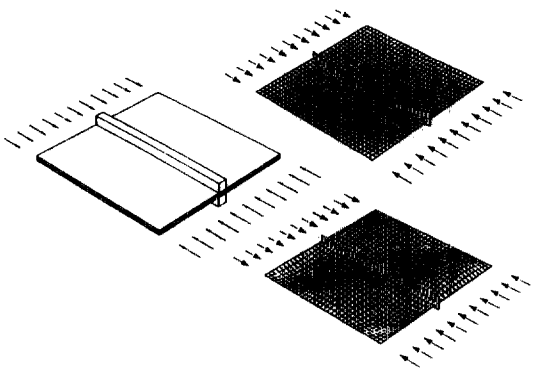

Fig. 4. Geometry and buckling modes of Case 2 for p=0.0002822.

ner and a weak plate so a much greater portion of the load is carried by the stiffener.

Case 2:
θ=0.04 and Ply Orientation (0^0Beam/0^0/90^0)s

For this configuration, only one optimum solution is found. It is listed in Table 2 below. The same results are presented graphically in Figure 5. It turns out to be the best design of those tested. Note that here the plate buckles simultaneously in all four modes.

Case 3:
θ=0.04 and Ply Orientation (90^0Beam/90^0/0^0)s

For this configuration, two different optimum solutions are found. They are listed in Table 3 below. The same results are presented graphically in Figures 6 and 7.

Of the two optima found, the global optimum occurs when three buckling modes occur simultaneously. No optimum was located that gave simultaneous buckling with all four modes. For this case, the stiffener fibers are in the 90^0 orientation so the stiffener adds much less stiffness to the plate than when the stiffener fibers are in the 0^0 orientation. Thus, most of the volume goes to the t_2(0^0 layer) and the t_1(90^0 layer) stays at the lower limit. Since there are only 3 desigh variables inactive from the bound constraints, it is impossible to obtain simultaneous buckling with all four modes. For the local optima case where p=0.

Table 2. Results of (0^0Beam/$0^0$$90^0$)s laminate for θ=0.04

t_1	t_2	b	h	p	Active Buckling Loads
0.00103	0.01385	0.06960	0.07350	0.0003949	P_1, P_2, P_3, P_5

Table 3. Results of (90^0Beam/90^0/0^0)s laminate for θ=0.04

t_1	t_2	b	h	p	Active Buckling Loads
0.00100	0.01900	0.00100	0.00100	0.0000677	P_1
0.00100	0.01538	0.02354	0.15323	0.0001804	P_1, P_2, P_3

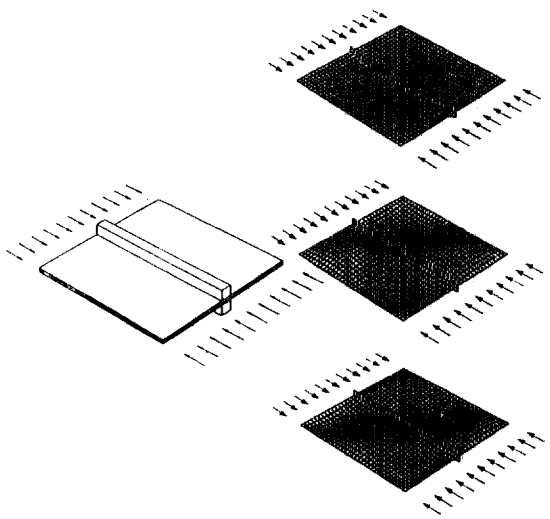

Fig. 5. Geometry and buckling modes of Case 2.

0000677, the stiffened plate is trying to reduce itself down to a single lamina with 0^0 fiber orientation. From this configuration, any incremental increase in the stiffener size causes a decrease in buckling load. By initially increasing the stiffener size, the load share carried by the stiffener, p_b, increases with the increase in the cross sectional area, s_b. The initial increase in p_b is greater than the increase in stiffness caused by the increase in s_b, therefore, the buckling load initially decreases creating the local optimum.

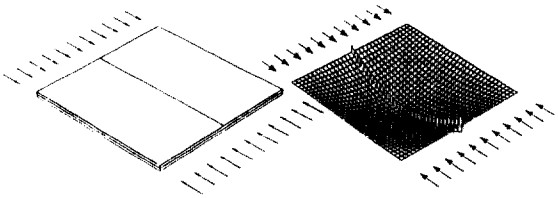

Fig. 6. Geometry and buckling mode of Case 3 for p=0.0000677.

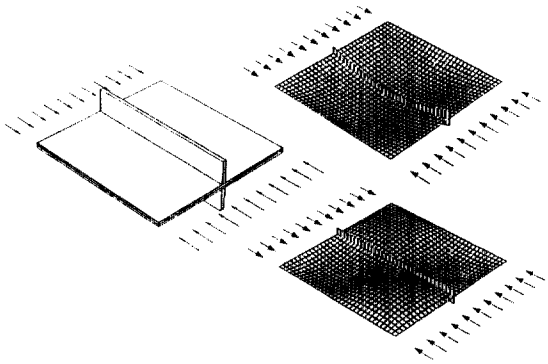

Fig. 7. Geometry and buckling modes of Case 3 for p=0.0001804.

Table 4. Results of (90°Beam/0°/90°)s laminate for θ=0.04

t_1	t_2	b	h	p	Active Buckling Loads
0.01900	0.00100	0.00100	0.00100	0.0000677	P_1
0.01636	0.00100	0.01845	0.14210	0.0001345	P_1, P_2, P_3
0.00778	0.00816	0.02830	0.14310	0.0001702	P_1, P_2, P_3, P_5

Case 4:

θ=0.04 and Ply Orientation (90°Beam/0°/90°)s

For this configuration, three different optimum solutions are found. They are listed in Table 4 below. The same results are presented graphically in Figures 8-10.

For this case, the global optimum occurs when all four buckling modes occur simultaneously. However, the buckling load of this global optimum is less than that of the global optimum of Case 3. It appears as though the inner layer t_2 is the preferred location for the 0° fibers. The configuration which gives p=0.0001345 corresponds closely to the Case 3 global optimum. The only difference is that more 0° fiber orientation volume is requi-

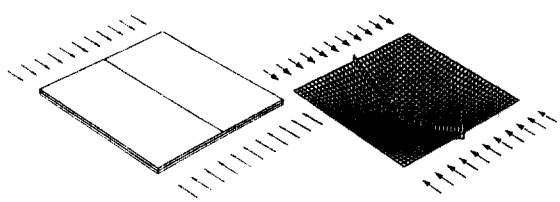

Fig. 8. Geometry and buckling mode of Case 4 for p=0.0000677.

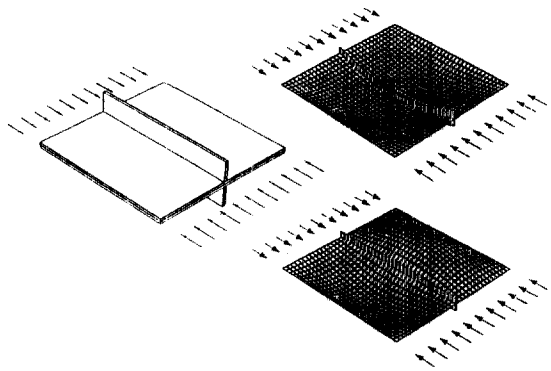

Fig. 9. Geometry and buckling modes of Case 4 for p=0.0001345.

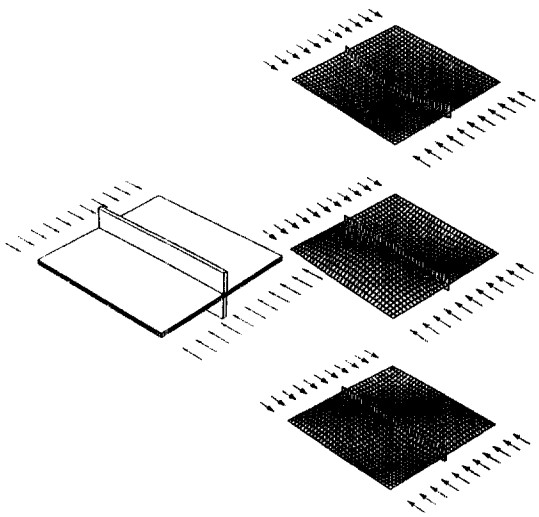

Fig. 10. Geometry and buckling modes of Case 4 for p=0.0001702.

red when it is located at the outer layer t_1. The local optimum, p=0.0000677, corresponds exactly to the Case 3 local optimum with the same load value. Here the same reasons apply for the existence of this local optimum.

Case 5:
θ=0.015 and Ply Orientation (0^0Beam/90^0/0^0)s

For this configuration, two optimum solutions are found. They are listed in Table 5 below. The same results are presented graphically in Figures 11 and 12.

Here the global optimum is found when the four buckling modes occur simultaneously. This global optimum corresponds to the global optimum found in Case 1. This follows since Case 5 is the same as Case 1, except for the smaller volume of material available. The local optimum found with p=0.0000124 is not unique. the total stiffener volume is uniquely defined but not the individual dimensions of the stiffener height and width. This is because the first buckling mode (the only active mode in this case) dose not cause any flexure of the stiffener so its cross sectional shape is not critical to the overall buckling stiffness.

Case 6:
θ=0.015 and Ply Orientation (0^0Beam/0^0/90^0)s

Table 5. Results of (0^0Beam/90^0/0^0)s laminate for θ=0.015

t_1	t_2	b	h	p	Active Buckling Loads
0.00298	0.00411	0.01008	0.04029	0.0000156	P_1, P_2, P_3, P_s
0.00576	0.00100	0.02720	0.02720	0.0000124	P_1

Table 6. Results of (0^0Beam/$0^0$$90^0$)s laminate for θ=0.015

t_1	t_2	b	h	p	Active Buckling Loads
0.00100	0.00577	0.01814	0.03986	0.0000179	P_1

For this configuration, only one optimum solution is found. It is listed in Table 6 below. The same results are presented graphically in Figure 13. This case is similar to Case 2 except here there is insufficient material available to produce simultaneous buckling of several modes.

The optima of Case 7 are closely related to the optima of Case 3. The only difference in the two cases is the total volume of material available. As in Case 3, here too, there is not sufficient material available to get the simultaneous buckling of all four modes.

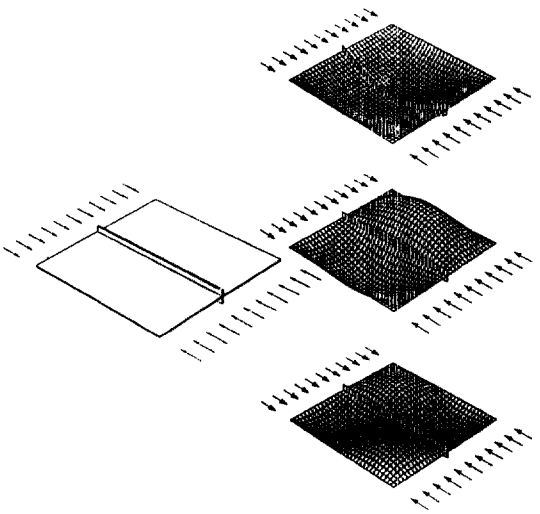

Fig. 11. Geometry and buckling mode of Case 5 for p=0.0000156.

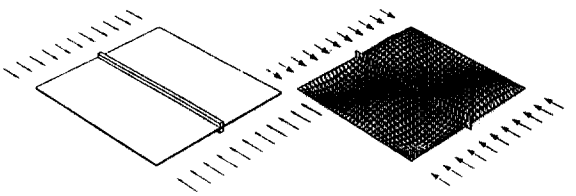

Fig. 12. Geometry and buckling modes of Case 5 for p=0.0000124.

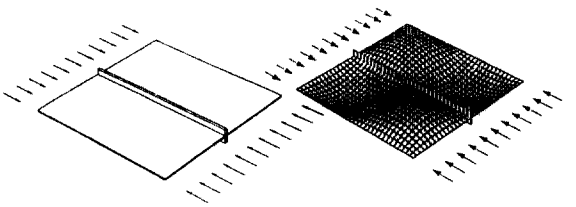

Fig. 13. Geometry and buckling mode of Case 6.

Case 7:

$\theta=0.015$ and Ply Orientation (90^0Beam/0^0/90^0)s

For this configuration, two different optimum solutions are found. They are listed in Table 8 below. The same results are presented graphically in Figures 16 and 17.

Case 8:

$\theta=0.015$ and Ply Orientation (90^0Beam/90^0/0^0)s

For this configuration, two different optimum solutions are found. They are listed in Table 7 below. The same results are presented graphically in Figures 14 and 15.

As in Case 4, the global optimum solution for Case 8 occurs when all four buckling modes occur simultaneously. Also there is a similar local optimum to that of Case 4, which has only one active buckling mode. One difference between Case 8 and Case 4 is that no local optimum in which three buckling modes occur simultaneously could

Table 7. Results of (90^0Beam/$90^0$$0^0$)s laminate for $\theta=0.015$

t_1	t_2	b	h	p	Active Buckling Loads
0.00100	0.00650	0.00100	0.00100	0.0000036	P_1
0.00100	0.00584	0.00669	0.09761	0.0000130	P_1, P_2, P_s

Table 8. Results of (90^0Beam/0^0/90^0)s laminate for $\theta=0.015$

t_1	t_2	b	h	p	Active Buckling Loads
0.00650	0.00100	0.00100	0.00100	0.0000036	P_1
0.00329	0.00345	0.00802	0.09386	0.0000125	P_1, P_2, P_3, P_s

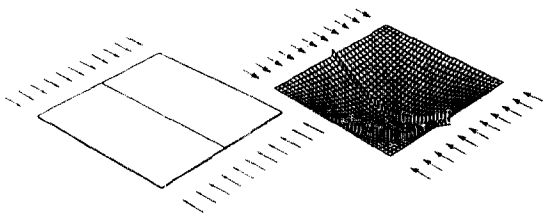

Fig. 16. Geometry and buckling mode of Case 8 for p=0.0000036.

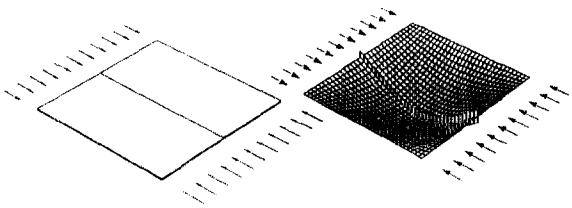

Fig. 14. Geometry and buckling mode of Case 7 for p=0.0000036.

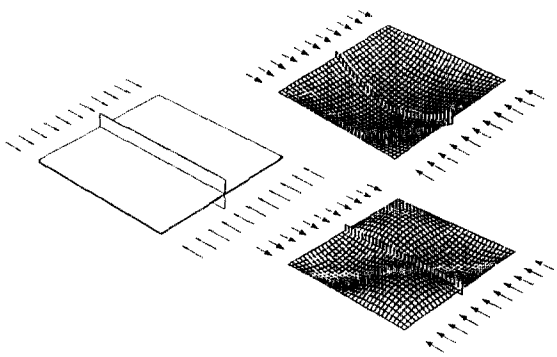

Fig. 15. Geometry and buckling modes of Case 7 for p=0.0000130.

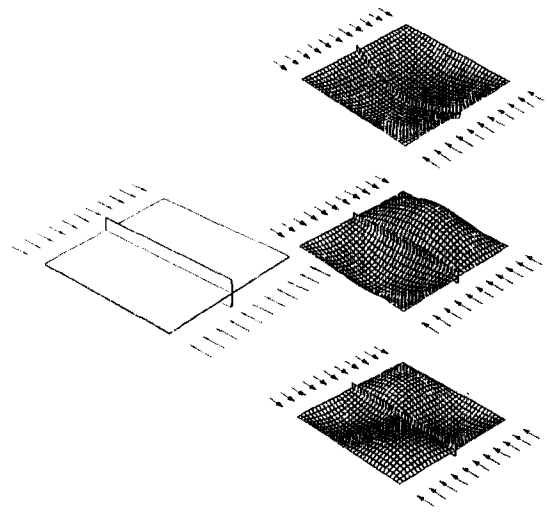

Fig. 17. Geometry and buckling modes of Case 8 for p=0.0000125.

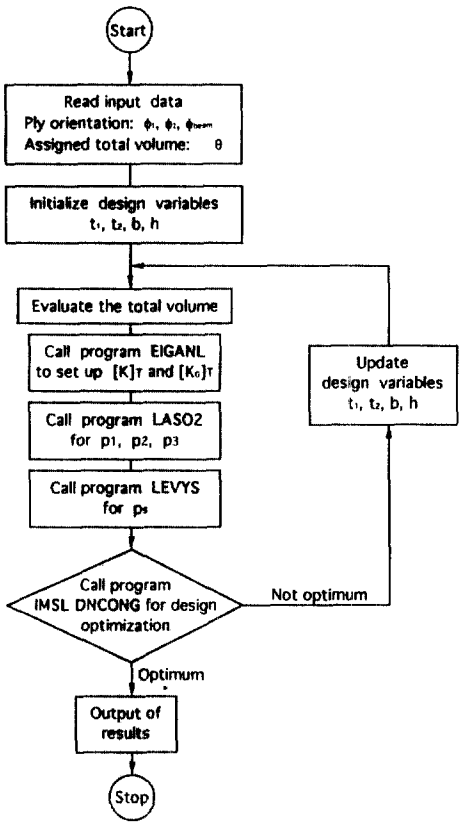

Fig. 18. Program flow chart.

be found for Case 8 as was found in Case 4.

Figure 18 shows the overall process of the program summarized in the form of a flow chart.

CONCLUDING REMARKS

The design optimization problem of the stiffened composite plate for maximum buckling load is a highly nonlinear problem. For almost all cases investigated, there were multiple optimum solutions. Some cases had as many as three different local optima. For both total volume constraints(θ= 0.04 and 0.015) examined, the best stacking configuration was the (0^0Beam/0^0/90^0)s used in cases 2 and 6. The use of 0^0 stiffener fiber orientation was always superior to 900 stiffener fiber orientation regardless of the laminae ply orientation. The laminae fiber orientation of ($0^0$$90^0$)s gives better results when used with 900 stiffener fiber orientation. However when used with 0^0 stiffener fiber orientation, the (90^0/0^0)s laminae fiber orientation was better.

ACKNOWLEDGMEMTS

This research was partly supported from the Ajou university in 1992. The financial assistance is gratefully acklowledged.

REFERENCES

1. Anderson, M. S., Stroud, W. J., Durling, B. J. and Hennessy, K.W., *"PASCO: Structural Panel Analysis and Sizing Code Users Manual,"* NASA TM-80182, 1981.
2. Bushnell, D. "PANDA2 - Program for Minimum Weight Design of Stiffened Composite, Locally Buckled Panels," *Comput. Struct.*, Vol. 25, pp. 469-605, 1987.
3. Swanson, G. D., and Gurdal, Z., "Structural Efficiency Study of Graphite-epoxy Aircraft Rib Structures," *AIAA/ASME/ASCE/AHS 29th Structures, Structural Dynamics, and Materials Conference*, Williamsburg, VA, April 18-20, pp. 85-97, 1988.
4. Shin, Y. S., "Optimal Design of Stiffened Laminated Plates Using a Homotopy Method," *AIAA/ASME/ASCE/AHS 32nd Structures, Structural Dynamics, and Materials Conference*, Baltimore, MD, April 8-10, 1991.
5. Yang, T. Y., *Finite Element Structural Analysis*, Prentice-Hall, Inc., Englewood Cliffs, NJ, 1986.
6. Scott, D. S. and Parlett, B. N., *"LASO2,"* NETLIB, Argonne National Lab., Argonne, IL, 1983.
7. Golub, G. H., Underwood, R., and Wilkinson, J. H., *"The Lanczos Algorithm for the Symmetric Ax* $=\lambda$ Bx Problem," Report STAN-CS-72-270,Depart-tment of Computer Science, Stanford University, Stanford, CA, 1972.
8. Jones, R. M., *Mechanics of Composite Materials*, McGraw-Hill Book Company, Washington, D.C., 1975.
9. Schittkowskl, K., *"NLPQL: A FORTRAN Subroutine Solving Constrained Nonlinear Programming Problems,"* Edited by Clyde L. Monma, Annals of Operational Research, Vol 5, pp. 485-500, 1985.

(接受 : 1992. 12. 28)